

See discussions, stats, and author profiles for this publication at: <https://www.researchgate.net/publication/265255825>

# Can Gap Tuning Schemes of Long-Range Corrected Hybrid Functionals Improve the Description of Hyperpolarizabilities?

ARTICLE in THE JOURNAL OF PHYSICAL CHEMISTRY B · SEPTEMBER 2014

Impact Factor: 3.3 · DOI: 10.1021/jp507226v · Source: PubMed

---

CITATIONS

8

---

READS

21

## 4 AUTHORS, INCLUDING:



[Osman Abdelkarim](#)

King Abdulaziz University

36 PUBLICATIONS 295 CITATIONS

[SEE PROFILE](#)



[Abdullah M. Asiri](#)

King Abdulaziz University

1,153 PUBLICATIONS 6,666 CITATIONS

[SEE PROFILE](#)

# Understanding the Origin of the Photocatalytic CO<sub>2</sub> Reduction by Au- and Cu-Loaded TiO<sub>2</sub>: A Microsecond Transient Absorption Spectroscopy Study

Herme G. Baldoví,<sup>†</sup> Ştefan Neaţu,<sup>†</sup> Anish Khan,<sup>‡,§</sup> Abdullah M. Asiri,<sup>‡,§</sup> Samia A. Kosa,<sup>‡,§</sup> and Hermenegildo Garcia\*,<sup>†,‡</sup>

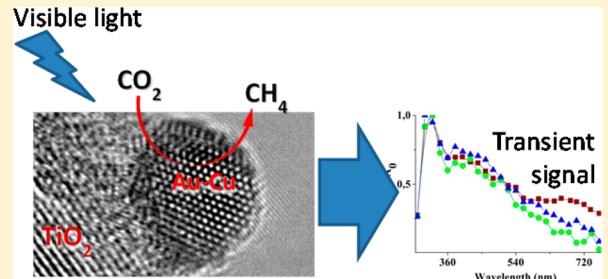
<sup>†</sup>Instituto Universitario de Tecnología Química, CSIC-UPV, and Departamento de Química, Universidad Politécnica de Valencia, Avd. de los Naranjos s/n, 46022, Valencia, Spain

<sup>‡</sup>Center of Excellence for Advanced Materials Research, King Abdulaziz University, Jeddah, Saudi Arabia

<sup>§</sup>Chemistry Department, Faculty of Science, King Abdulaziz University, Jeddah 21589, Saudi Arabia

## S Supporting Information

**ABSTRACT:** Recent photocatalytic data for CO<sub>2</sub> reduction by H<sub>2</sub>O using simulated sunlight have shown that, while TiO<sub>2</sub> Evonik P25 containing Au nanoparticles (NPs; Au/P25) generates considerably higher amounts of hydrogen than methane, when P25 contains Au–Cu alloy NPs the selectivity toward methane increases dramatically. To gain insight into this photocatalytic behavior, in the present work we have performed a transient absorption spectroscopy study in the microsecond time scale of three samples, namely, Au/P25, Cu/P25, and (Au, Cu)/P25 using 355 (UV) and 532 nm (visible) lasers. The transient spectra exhibit as common features a narrower peak at about 320 nm and a broad band from 400 to 800 nm. Using oxygen as electron quencher and methanol as hole quencher, the transient signals have been assigned to charge separation. Several cases were observed, including: (i) absence of quenching attributed to the lack of accessibility of the quencher to the site, (ii) quenching of the signal, or (iii) increase of the transient signal intensity attributed to less charge recombination by removal of one of the charge carriers. Of relevance to understand the origin of the photocatalytic CO<sub>2</sub> reduction by H<sub>2</sub>O is the quenching of the charge separated state by these two reagents. In this way, it was observed that H<sub>2</sub>O exerts a remarkable influence to the transient signal, quenching its intensity in the three samples at the two irradiation wavelengths, except for (Au, Cu)/P25 upon 532 nm excitation. Importantly, the distinctive behavior due to the presence of Cu has been attributed to the observed quenching by CO<sub>2</sub> of the broad 400–800 nm band when excitation is performed with UV 355 nm light.



## INTRODUCTION

Photocatalysis is attracting a renewed interest because, in addition to environment remediation, it is being increasingly considered as a potential alternative for the production of solar fuels.<sup>1–5</sup> Besides hydrogen generation from water, another topic that is under the spotlight is the photocatalytic reduction of CO<sub>2</sub>.<sup>1–9</sup> Due to the technological problems associated with the room temperature hydrogen storage,<sup>10–12</sup> fuels delivered from CO<sub>2</sub>, such as methane and methanol, could be readily applicable with minor changes as current energy sources.<sup>13–17</sup>

In this context, there are several open issues in photocatalytic CO<sub>2</sub> reduction including the three major ones of (i) increasing the efficiency of the photocatalyst, (ii) how to control the activity toward selective CO<sub>2</sub> reduction in the presence of water, and (iii) how to direct the process toward a single product formation.<sup>16</sup> In the photocatalytic CO<sub>2</sub> reduction, water is considered the ideal reducing agent, providing electrons and protons to CO<sub>2</sub>, the problem being to promote CO<sub>2</sub> reduction without generating hydrogen predominantly.<sup>9,16</sup>

One general methodology to increase the efficiency of a metal oxide semiconductor as photocatalyst is the deposition on its surface of NPs as cocatalysts. These cocatalysts should act as reservoirs of charges and catalytic centers for the interaction of these charges with the chemical substrate. Noble metal NPs, such as platinum or gold, have been used as cocatalysts for hydrogen generation from water.<sup>18</sup> Recently, we have reported that due to the presence of the plasmon surface band, another effect of Au NPs is the introduction, specifically by this metal, of visible light photoresponse in TiO<sub>2</sub>.<sup>19</sup> A logical extension of the use of Au/P25 as photocatalyst would be to test its performance for CO<sub>2</sub> reduction by water. However, preliminary tests have shown that H<sub>2</sub> generation is the major product of the reduction, accompanied by less amounts of methane. In the field of photocatalytic CO<sub>2</sub> reduction, it is well-known that the

Received: October 22, 2014

Revised: March 3, 2015

Published: March 3, 2015

presence of Cu exerts a notable influence on the product selectivity, favoring the formation of methane with respect to other possible products and particularly CO.<sup>20</sup> In view of these precedents, we have recently evaluated the photocatalytic activity of TiO<sub>2</sub> supporting in appropriate proportions Au and Cu NPs as cocatalyst [(Au, Cu)/TiO<sub>2</sub>] and found that in this system the presence of Cu minimizes dramatically H<sub>2</sub> production, leading to methane in high selectivity and rendering one of the most efficient photocatalyst for CO<sub>2</sub> reduction by water ever reported, with a maximum methane production rate about 2000 μmol g<sup>-1</sup> h<sup>-1</sup> under simulated sunlight irradiation.<sup>21</sup>

Unfortunately, there is a lack of understanding of the origin of the effect caused by the presence of Cu that limits further advances in the area. Insights into the role of Cu and the operation of the (Au, Cu)/TiO<sub>2</sub> can be obtained by a combination of theoretic calculations and modeling with experimental techniques trying to detect different species that can serve to rationalize the role of Cu in the behavior of photocatalysts. The present manuscript presents transient absorption spectroscopy (TAS) data showing that the differences in the product selectivity, due to the presence of Cu, of the TiO<sub>2</sub> photocatalysts are also reflected in TAS and, more importantly, on the quenching behavior of the charge separated state.

TAS techniques are powerful spectroscopy methods to detect and follow the reactivity of transients species generated upon photon absorption. In the field of photocatalysis, TAS has found limited applications due to the complexity of the photocatalytic events and also because metal oxide semiconductors are opaque solids that require the use of the diffuse reflectance (for thick beds) or transmission (for thin micrometer film) techniques. These conditions are, however, far from photocatalytic reactions in which frequently suspended NPs are in contact with a liquid or a gas phase. Recently, we have reported a new methodology for TAS based on application of transmission mode to diluted persistent suspensions of photocatalyst NPs.<sup>22</sup> Due to the small particle sizes of most of the current photocatalysts and, particularly, TiO<sub>2</sub>, it is possible to prepare by sonication colloidal suspensions of these NPs that are persistent and suitable for TAS measurements by transmission. In the present study, we have applied this methodology to obtain, under various conditions, TAS of TiO<sub>2</sub> samples modified or not by the presence of Au or Cu NPs using a nanosecond laser pulse and monitoring the signal in the microsecond time scale. The results obtained show sufficient similarities and other differences between these photocatalysts to propose the origin of the effect of Cu on TiO<sub>2</sub> photocatalysts. Quenching of the charge separated state by CO<sub>2</sub> and simultaneous CH<sub>4</sub> formation has been only observed for (Au,Cu)/P25, showing that TAS can report on the contrasting behavior of modified titania samples. The information obtained can be relevant for the design of more advanced TiO<sub>2</sub>-based photocatalyst for CO<sub>2</sub> reduction by H<sub>2</sub>O.

## ■ EXPERIMENTAL SECTION

**Sample Preparation.** Sample preparation and the characterization of the samples under study have already been reported in ref 21. Briefly, the synthesis starts from the commercial TiO<sub>2</sub> (Evonik P25) used as support. Au/P25 was prepared following the so-called deposition–precipitation method. This procedure renders a photocatalyst containing 1.5 wt % of Au in the form of NPs with a narrow size

distribution about 5 nm. Cu/P25 was obtained following also an analogous deposition–precipitation method starting from Cu(NO<sub>3</sub>)<sub>2</sub> in aqueous solution at pH 9 for the deposition step. Both the Au and the Cu reduction was carried out by treating the sample at 400 °C under a H<sub>2</sub> atmosphere. The Cu content was 1.5 wt %. A third sample containing Au–Cu alloy NPs, (Au, Cu)/P25, was obtained by consecutive independent deposition, first of Au (0.5 wt %) and second of Cu (1 wt %), followed by a final thermal reduction treatment with H<sub>2</sub>.

**TAS Measurements.** The solvents were provided by Sharlau and the precursor P25 was supplied by Evonik, while the rest of chemicals used, including HAuCl<sub>4</sub> and Cu(NO<sub>3</sub>)<sub>2</sub>, were acquired from Sigma-Aldrich. The solid powders (1.5 mg) have been suspended in dry acetonitrile (5 mL) by sonication, and the resulting suspensions, after separation of any solid residue, were subjected to TAS in transmission mode. TAS measurements have been performed using as excitation sources the third (355 nm) harmonic of a Surelite Nd:YAG laser (20 mJ, pulse ≤10 ns) and 532 nm Lotis laser (35 mJ, pulse 7 ≤ns). Laser power dependency on the transient signal intensity and decay was studied in the power range of 24–60 and 33–70 mJ for 355 and 532 nm laser, respectively. A Tektronix 2440 digitizer captures the signal from the monochromator/photomultiplier detection system and transfers it to a PC computer. The time resolution of the system is limited by the response of the photomultiplier that is in the range of tens of ns. Thus, the laser flash is considered to be instantaneous in the time scale of μs in which the signal is being monitored. O<sub>2</sub> quenching was performed by flowing an O<sub>2</sub> stream through the bottom in the 1 cm × 1 cm quartz cells at least 5 min before measurements by connecting with a syringe a balloon full with O<sub>2</sub> with the cells capped with a septum. CO<sub>2</sub> quenching was carried out similarly, but the purging was performed with 99% pure CO<sub>2</sub> instead of O<sub>2</sub>. Methanol and H<sub>2</sub>O quenching was carried out by injecting with a syringe 10 μL of 99% methanol into a septum capped in 3 mL quartz cells containing the suspended photocatalyst in acetonitrile.

**UV-vis Spectroscopy Measurements.** UV-visible absorption spectra were recorded with a Jasco V-650. The solvent used in all measurements was dry acetonitrile, and the spectra were recorded using 10 mm × 10 mm quartz cells with 4 mL capacity.

**Photocatalytic Tests.** A thin layer of the photocatalyst was placed inside the photoreactor filled with CO<sub>2</sub>/H<sub>2</sub>O diluted with N<sub>2</sub> and irradiated with a solar simulator at 60 °C, as indicated in ref 21. The course of the reaction was followed by analyzing periodically the gas phase by directly coupling the photoreactor to a dual-channel gas chromatograph (Agilent Technology 490 Micro GC) equipped with MSSA and PPQ columns and two TCDs.

## ■ RESULTS AND DISCUSSION

In the present study, we have prepared three different TiO<sub>2</sub> samples that have been submitted to 355 or 532 nm laser flash. Specifically, the commercial P25 has been modified by addition of Au NPs, Cu NPs, or (Au, Cu) NPs.

Table 1 summarizes the main analytical properties for the samples under study. It should be noted that the metal content and particle size of the metal were similar in these three samples. Au was deposited on TiO<sub>2</sub> P25 following the so-called deposition-precipitation method followed by reduction of the deposited metal with H<sub>2</sub> at 400 °C. The (Au, Cu)/TiO<sub>2</sub> P25 was prepared starting with the deposition of Au and then

**Table 1. Main Analytical and Photocatalytic Properties of the Samples under Study**

sample	metal loading <sup>a</sup> (wt %)	metal particle size <sup>b</sup> (nm)	CH <sub>4</sub> formation rates <sup>c,d</sup> (μmol/g × h)
P25	0		0
Au/P25	1.5	5	210
Cu/P25	1.5	5	280
(Au, Cu)/P25	1.5 (Au/Cu = 1 : 2)	5	2200

<sup>a</sup>ICP-OES measurements. <sup>b</sup>HRTEM measurements. <sup>c</sup>Data taken from ref 21. <sup>d</sup>Controls in the absence of light or irradiating in the presence of photocatalyst in the absence of CO<sub>2</sub> showed no CH<sub>4</sub> formation.

followed by the Cu deposition using Cu(NO<sub>3</sub>)<sub>2</sub> and reduced with H<sub>2</sub>. Figure 1 presents the diffuse-reflectance UV-vis

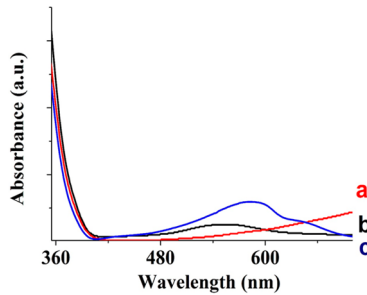


**Figure 1.** Diffuse reflectance UV-vis spectra of Cu/P25 (a), Au/P25 (b), and (Au, Cu)/P25 (c).

absorption spectra of Au/P25, Cu/P25, and (Au, Cu)/P25 showing the band in the visible region peaking around 560 nm

due to Au surface plasmon band and an additional peak at 650 nm due to the presence of Cu.

These three samples exhibit very different photocatalytic activity for the reduction of CO<sub>2</sub> by water (see Table 1).<sup>21</sup> While Au/P25 under simulated sunlight generates H<sub>2</sub> accompanied by minor amounts of methane, the (Au, Cu)/P25 exhibits an optimal photocatalytic activity for CO<sub>2</sub> reduction by water.<sup>21</sup> The Cu/P25 sample exhibits a good photocatalytic activity in this process. With these precedents in mind, we performed TAS experiments under UV (355 nm) and visible-light (532 nm) laser irradiation. These two wavelengths were selected because they should excite specifically P25 (355 nm) or the metal NPs (532 nm). It should be noted that excitation in the UV should take place predominantly on the P25 semiconductor and that under these conditions metal NPs can act in various ways, including as electron reservoirs of CB electrons from the P25 and as catalytic sites for gas evolution. The 532 nm excitation should promote mainly electrons from metal NPs to the conduction band of the semiconductor.

In the following sections, we first discuss TAS upon 355 nm excitation and separately in another section the transients recorded upon 532 nm excitation. In all cases, the photocatalysts were suspended in acetonitrile by sonication and removal of solid residues, rendering a clear colloidal suspension. Due to the particle size of the photocatalysts, these colloidal suspensions were indefinitely persistent for periods of time much longer than the time required for TAS measurements (about 3 h), without observing the formation of any solid or appearance of turbidity. Dynamic laser scattering shows that the apparent particle size in the colloidal suspensions was 50–100 nm. We have to note that during extended exposure to the laser flash the average particle size decreased to 20–50 nm.<sup>22</sup> Chemical analyses of Au and Cu of the supernatant after removal of the solids by filtration of suspensions that have been submitted to the TAS study showed that the percentage of Au

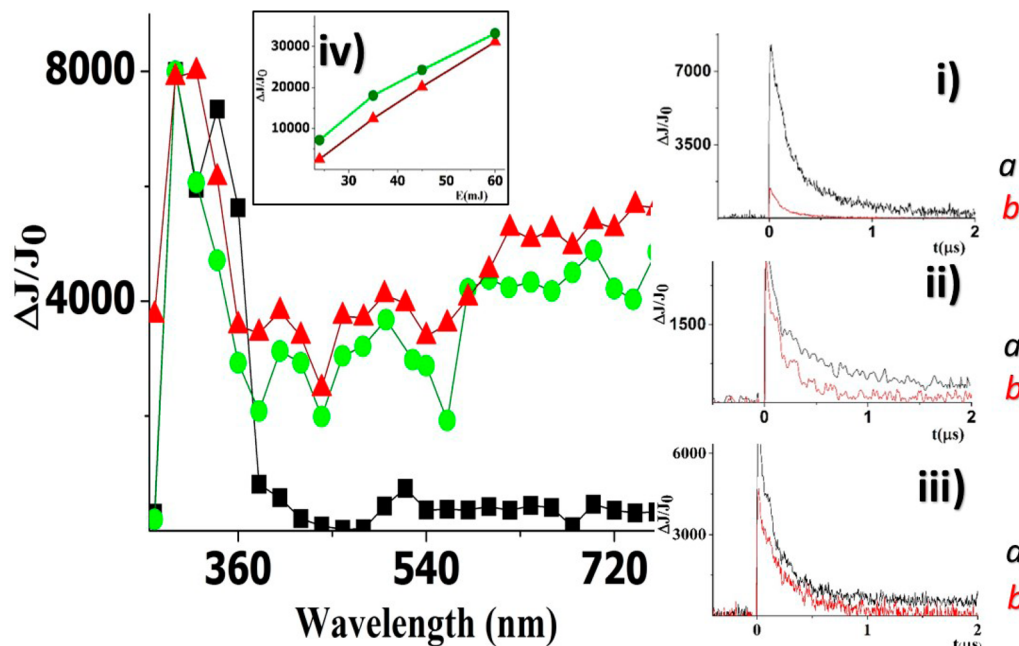


**Figure 2.** Transient spectra recorded 160 ns after 355 nm laser flash for Ar purged P25 (black square), Au/P25 (red triangle), and Cu/P25 (green circle) samples. Insets i, ii, and iii show the temporal profiles of the signal monitored at 320 (a) and 720 nm (b) for P25, Au/P25, and Cu/P25, respectively. Inset iv shows the dependency of the signal intensity with the laser power for Au/P25 (red triangle) and Cu/P25 (green circle), respectively.

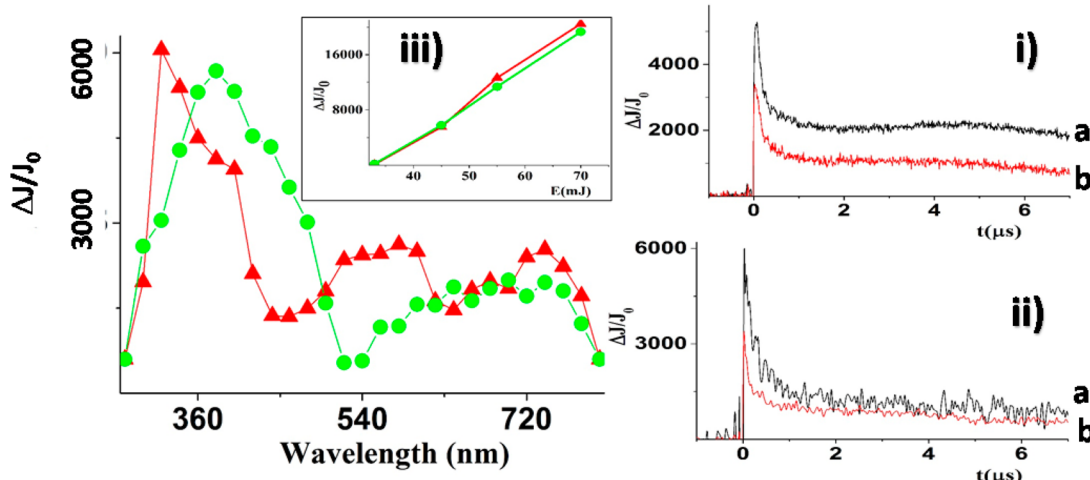


**Figure 3.** Transient spectra of Ar-purged Au/P25 (green circle) and Cu/P25 (red triangle) recorded 300 ns after 532 nm laser excitation (7 ns fwhp,  $35 \text{ mJ} \times \text{pulse}^{-1}$ ). The insets i and ii show the transient signal monitored at 320 (a) and 720 nm (b) for Au/P25 (i) and Cu/P25 (ii). Inset iii plots the dependency of the initial signal intensity with the laser power for Au/P25 (green circle) and Cu/P25 (red triangle), respectively.

was under the detection limit (10 ppb) and that the amount of Cu leached is negligible (0.4% of the initial amount present on Cu/P25). Controls submitting to TAS study a solution of  $\text{Cu(OAc)}_2$  in acetonitrile at submicromolar concentrations ( $0.3 \mu\text{M}$ ) corresponding to the leached Cu did not allow to detect any transient signal.

In the next section, data corresponding to the Au/P25 and Cu/P25 samples will be first presented. Then, after showing similarities and differences between these two photocatalysts, the case of (Au, Cu)/P25 will be described and commented with the aim of gaining understanding on the unique synergy of the Au–Cu alloy for the photocatalytic  $\text{CO}_2$  reduction.

**TAS Recorded at 355 nm.** Upon laser excitation at 355 nm, P25 exhibits a sharp absorption peak at  $\lambda_{\text{max}} 340 \text{ nm}$ . The signal is short-lived and decays completely in  $2 \mu\text{s}$  after the laser flash. The best fitting of the signal temporal profile to monoexponential decay gives a lifetime of 60 ns. In contrast to the behavior of P25, both Au/P25 and Cu/P25 exhibit a very similar transient absorption spectrum characterized by a sharp absorption band at  $\lambda_{\text{max}} 320 \text{ nm}$ , similar to P25, accompanied by a very broad absorption spanning from 400 to 800 nm, which grows in intensity toward the red, with a lifetime of 200 ns, approximately. The temporal profile of the signal in this broad band was coincident in all the wavelengths for the case of Au/P25 and Cu/P25, but it was somehow shorter lived than the signal monitored at 320 nm. The influence of the laser power in the range from 20 to  $60 \text{ mJ} \times \text{pulse}^{-1}$  shows that the signal intensity grows linearly with the laser power and that the decay of the signal remains constant in this power range. Figure 2 presents the transient absorption spectra for these three samples recorded 160 ns after excitation in the UV and a set of representative transient decays for each sample. The influence of the signal intensity versus the laser power is also presented as an inset in Figure 2.

Considering the well-known behavior of  $\text{TiO}_2$  photocatalysts, that upon light excitation lead to charge separation with generation of electrons in the conduction band (CB) and holes in the valence band (VB), it can be assumed that the transients shown in Figure 2 could correspond to those families of the charge separated state, probably located in trapping sites, having the longest lifetime. In order to provide some evidence in support of this assignment, the quenching behavior of this

transient signal by oxygen and methanol, as electron acceptor and electron donor quenchers, respectively, was studied. The quenching behavior can be rationalized fully satisfactorily based on this assumption that the signal monitored corresponds to the state of charge separation with electrons and holes located at different trapping sites on the particles. Thus, it was observed that, for Au/P25, both quenchers increase significantly the intensity of the top  $\Delta J/J_0$ , while on the other hand, the presence of quenchers decreases the lifetime of the signal (see Supporting Information, Figures S1–S3). This quenching behavior was observed monitoring both at 330 and at 720 nm, that were taken as representative wavelengths for the sharp, defined peak and for the broad 400–800 nm band, respectively.

We interpreted these results considering that the presence of the quencher should reduce prompt charge recombination, thus, leading to an increase of the initial  $\Delta J/J_0$  intensity of the complementary charge carrier. The fact that both oxygen and methanol behave similarly indicates that the TAS corresponds to a charge separation state, combining the absorption of both electron and holes. The decay of the signal in the presence of the quenchers was somewhat faster than in the absence, indicating that, besides increasing the intensity of the charge separation state immediately after laser pulse, the quenchers can access to some of the charge carriers increasing their decay in submicrosecond time scale.

The behavior of Cu/P25 contrasts with that just commented for Au/P25. In the Cu/P25 case, the signal at 320 nm is insensitive, both in the value of top  $\Delta J/J_0$  and in the temporal profile of the signal, to the presence of  $\text{O}_2$  or  $\text{CH}_3\text{OH}$  quenchers. In contrast, the broad band from 400 to 800 nm for the transient spectrum of Cu/P25 becomes quenched both by methanol and oxygen without any increase of the top  $\Delta J/J_0$ . Thus, it seems that in the case of Cu/P25, the charge separated state is better protected from quenchers than in the case of Au/P25 and, for this reason, there is not an increase of the intensity of the value of the top  $\Delta J/J_0$ . Only at longer time scales there is a dynamic quenching in the broad 400–800 nm band for both quenchers, resulting in a faster signal. These observations suggest that the state of charge separation is less accessible in Cu/P25 than in the case of Au/P25. It should be noted that the 400–800 nm band present in both Au/P25 and Cu/P25 samples is sensitive to the presence of quenchers, although

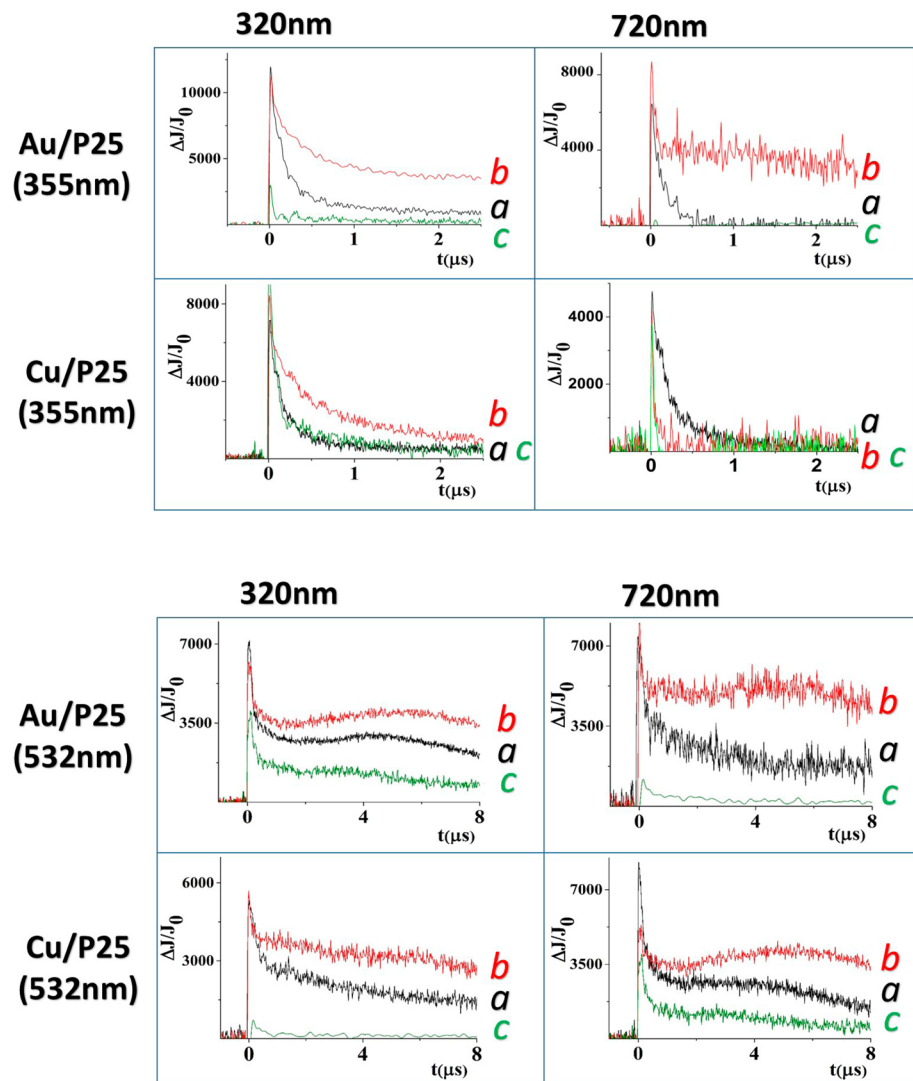


**Figure 4.** Temporal profile of the signals monitored at 320 (left) or 700 (right) nm under an Ar (a) atmosphere or quenched by  $\text{CO}_2$  (b) or  $\text{H}_2\text{O}$  (c) as a function of the excitation wavelengths (355 or 532 nm laser) for Au/P25 and Cu/P25.

differently depending on the metal NPs. This band is absent in the transient absorption spectrum of P25, reflecting in this way the influence that the minor percentages of metals (1.5 wt %) can have in the photocatalytic activity of  $\text{TiO}_2$ .

**TAS upon Green Light (532 nm) Excitation.** P25 does not exhibit any TAS upon excitation in the visible region, which is in agreement with the well-known lack of photoresponse of titania photocatalysts under visible light irradiation. In contrast, Au/P25 and Cu/P25 exhibit upon 532 nm laser excitation TAS that are similar to those previously recorded under UV light, except that the peak at 320 nm becomes broader and less intense. Also at 532, a linear relationship between the signal intensity and the laser power in the range from 33 to 70  $\text{mJ} \times \text{pulse}^{-1}$  without alteration of the temporal decay was observed for Au/P25 and Cu/P25. Figure 3 shows TAS recorded for these two metal containing P25 photocatalysts as well as a temporal profile of the signal monitored at 320 and 720 nm. Inset c presents the influence of the initial signal intensity as a function of the laser power.

Although TAS of Au/P25 and Cu/P25 were similar, the transient decays exhibit some differences. In the case of Au/P25, the signal monitored at 320 nm presents three regimes

corresponding to an initial fast decay being complete in less than 1  $\mu\text{s}$ , which is approximately 55% from the initial  $\Delta J/J_0$  intensity. This fast decay is followed by a growth of the signal intensity from 1 to 5  $\mu\text{s}$ , leading to an increase about 10%. The third regime corresponds to the final decay of the transient signal. The signal monitored at 720 nm for Au/P25 also presents these three regimes, but the percentage of the initial decay is larger (60%), and the growth of the signal is smaller (5%). We attribute the growth observed in the transient signal from 1 to 5  $\mu\text{s}$ , as reflecting a delayed generation of charge separated states, due to the migration of charge carriers and relocation in traps having longer lifetime and higher absorptivity. According to previous studies, this relocation can be caused by the migration of electrons from Au NPs to P25 conduction band.<sup>23,24</sup> In the case of Cu/P25, the temporal profiles did not exhibit any growth in the signal, but the two different regimes, fast and slow, are still observed (see Figure 3, inset b).

Assignment of the transient spectra upon 532 nm also to the charge separation states was based on the influence of both oxygen and methanol quenchers on the signal. Again, contrasting quenching behavior between Au/P25 and Cu/

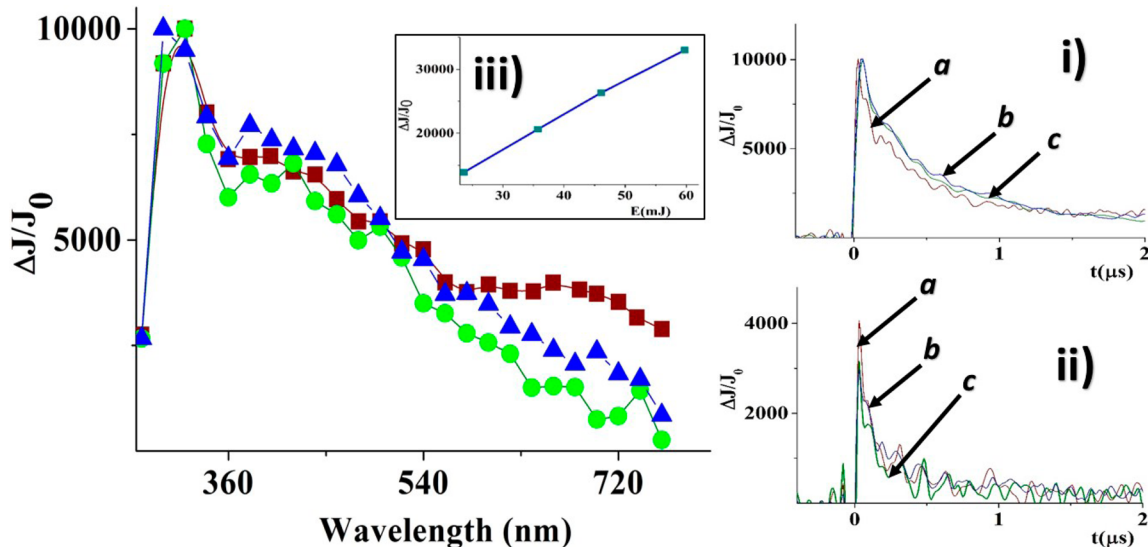


**Figure 5.** Transient spectra of (Au, Cu)/P25 recorded 160 ns after 355 nm laser excitation of Ar purged sample (red square) or after O<sub>2</sub> (blue diamond) or MeOH (green circle) quenching. The insets i and ii show the transient signals monitored at 320 (i) and 720 nm (ii) for (Au, Cu)/P25 under Ar (a) or O<sub>2</sub> (b) atmosphere or after MeOH quenching (c). Inset c shows the power dependency of the initial transient signal.

P25 was observed (see Supporting Information, Figures S4–S5). In the case of Au/P25, both oxygen and methanol lead to a decrease of the top of  $\Delta J/J_0$  value and a decrease in the lifetime of the signal. Again, the fact that both oxygen and methanol exhibit the same effect indicates that the transient spectra correspond to the state of charge separation with the combined absorption of electrons and holes in the same wavelength range.

In the case of Cu/P25, the transient signal monitored at 320 nm increases in the initial  $\Delta J/J_0$  intensity, both in the presence of oxygen or methanol, corresponding to a charge separation state, but responding immediately to the presence of quenchers in the subnanosecond time scale. It was interesting to observe a specific quenching behavior for the broad 400–800 nm band of Cu/P25 upon 532 nm excitation, which was different from the quenching response of the other materials at other wavelengths. In this case, methanol does not quench the signal and the temporal profile does not undergo any alteration due its presence. In contrast, in this wavelength region upon this excitation, oxygen decreases significantly the initial  $\Delta J/J_0$  value of the signal. According to this response, for the case of Cu/P25 photocatalyst upon visible light excitation, the transient signal in this spectral region should be attributed to electrons located on the surface of Cu/P25 semiconductor accessible to methanol and oxygen. Overall, the contrasting behavior of the transient signals for Au/P25 and Cu/P25, depending on the UV or visible excitation, and the absence of photoresponse of P25 at 532 nm excitation provides sufficient evidence that the irradiation at 532 nm leads to excitation of the metal NPs, while in the case of irradiation at 355 nm, the predominant photoresponse should be at P25 semiconductor. In addition, the summary of oxygen or methanol quenching process is that all the transient signals correspond to the combined absorption of electrons and holes, except in the case of Cu/P25 at 532 nm excitation, where the 400–800 nm band behaves like CB electrons. Also notable is the fact that a decrease in the intensity of the  $\Delta J/J_0$  signal immediately after the laser flash, attributable to static quenching, is observed for Au/P25 at 355 nm irradiation, but not at 532 nm. The reverse behavior of the variation of the initial  $\Delta J/J_0$  intensity happens for Cu/P25. Overall, the present data firmly proves that metal NPs

deposited on P25 play a decisive influence on the behavior and lifetime of the charge separated state and that this influence can be monitored by TAS.

**Quenching by CO<sub>2</sub> and H<sub>2</sub>O.** As commented in the Introduction, the main purpose of this transient absorption study is to provide understanding on the influence that the presence of Au–Cu alloy NPs plays on the photocatalytic activity of the CO<sub>2</sub> reduction by water. Under the conditions of the photocatalytic CO<sub>2</sub> reduction, Au/P25 forms preferentially H<sub>2</sub>, while the presence of Cu alloying Au NPs directs the selectivity of (Au, Cu)/P25 toward methane formation.<sup>21</sup> To provide some spectroscopic data that could shed light on this contrasting behavior, quenching experiments of the transient signal for P25, Au/P25, Cu/P25 and (Au, Cu)/P25 both under 355 and 532 nm irradiation by CO<sub>2</sub> and H<sub>2</sub>O were performed. A summary of the results is presented in Figure 4.

As it can be seen in Figure 4, in all the cases except Cu/P25 at 355 nm, regardless of excitation light or photocatalyst, the presence of water results in quenching of the signal in both the short and the long wavelength of TAS. This signal quenching is understandable since water adsorbs strongly on the surface of TiO<sub>2</sub> and can act as hole and electron quencher. Similarly, in all cases except Cu/P25 at 355 nm irradiation, the presence of CO<sub>2</sub> increases the lifetime of the signal monitored at any wavelength in the spectrum, even in the case of Au/P25 upon 532 nm irradiation. It is difficult to rationalize how the presence of CO<sub>2</sub> increases the lifetime of charge separation, but probably this effect arises from the strong interaction of acidic CO<sub>2</sub> with basic sites on the semiconductor surface.<sup>25,26</sup> It has been extensively documented that CO<sub>2</sub> adsorption on the surface of metal oxides leads to the formation of hydrogen carbonate and carbonates.<sup>27–29</sup> In the case of TiO<sub>2</sub>, and particularly P25, all these species have been detected by FTIR spectroscopy.<sup>21</sup> It is very likely that the sites of CO<sub>2</sub> adsorption are also the sites that promote e<sup>−</sup>/h<sup>+</sup> recombination at the surface of the solid. By masking these recombination sites due to neutralization by CO<sub>2</sub>, the initial intensity of the  $\Delta J/J_0$  signals and their lifetime would increase. It has to be, however, commented that this increase in the intensity and lifetime of charge separation by

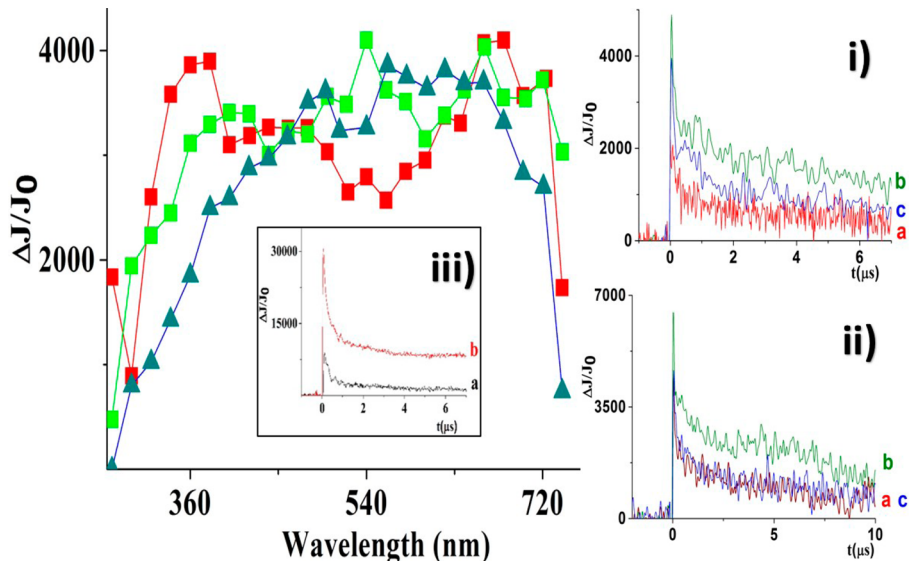


**Figure 6.** Transient spectra of (Au, Cu)/P25 recorded 300 ns after 532 nm (7 ns fwhp,  $35 \text{ mJ} \times \text{pulse}^{-1}$ ) laser excitation of samples under Ar purging (red square) or after  $\text{O}_2$  (blue diamond) or MeOH (green square) quenching. The insets i and ii show the transient signals monitored at 320 (i) and 720 nm (ii) for (Au, Cu)/P25 under Ar (a) or after MeOH (b) and  $\text{O}_2$  (c) quenching. Inset iii shows the decay of the transient signal monitored at 480 nm recorded at 45 (a) and 75 (b)  $\text{mJ} \times \text{pulse}^{-1}$ , respectively.

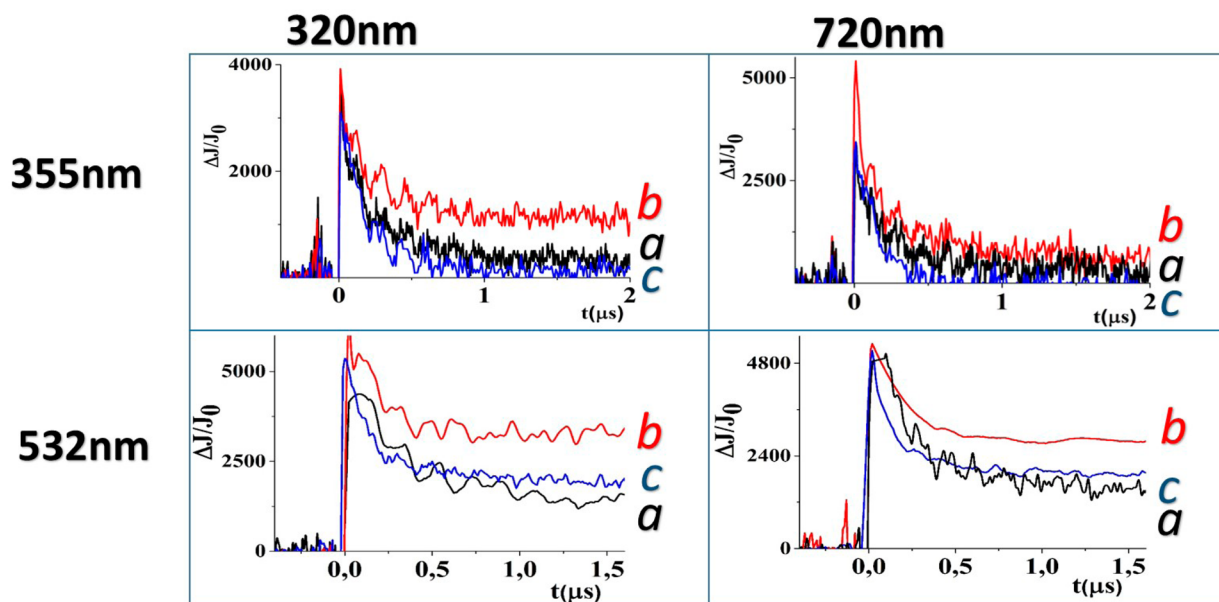


**Figure 7.** Temporal profile of the signals monitored at 320 (left) or 720 (right) nm under an Ar atmosphere (a), quenched by  $\text{CO}_2$  (b) or  $\text{H}_2\text{O}$  (c) as a function of the excitation wavelengths (355 or 532 nm laser) for (Au, Cu)/P25.

$\text{CO}_2$  adsorption is more notable for Au/P25 compared to Cu/P25 in the case of 355 nm irradiation.

The only exception to this rule of higher intensity and longer lifetime of charge separation by the effect of  $\text{CO}_2$  was observed for the case of UV light (355 nm) excitation of Cu/P25. In this sole case, quenching of the transient signal by the presence of  $\text{CO}_2$  was observed only monitoring in the 400–800 nm region. Based on this unique behavior with regard to  $\text{CO}_2$ , it can be proposed that the broad band from 400 to 800 nm, corresponding to electrons upon UV radiation probably originated by  $\text{TiO}_2$  excitation rather than excitation of the metal NPs, are the transients responsible for the transformation of  $\text{CO}_2$  to methane, since this is the only signal that apparently reacts with  $\text{CO}_2$ . This hypothesis was supported by the

observation of methane evolution upon 355 nm excitation of Cu/P25, where  $\text{CO}_2$  quenching is observed, while no methane was detected when Cu/P25 was excited at 532 nm, where no  $\text{CO}_2$  quenching is detected by TAS.

**TAS Recorded for (Au, Cu)/P25.** The sample that has exhibited the highest photocatalytic activity for  $\text{CO}_2$  reduction by water is in fact a P25 that contains simultaneously Au and Cu alloyed NPs prepared by consecutive deposition first of Au and subsequently Cu (see Experimental Section for preparation of the sample and Table 1 for photocatalytic data). Therefore, it is important to study the photochemical response of (Au, Cu)/P25, particularly with regard to  $\text{CO}_2$  interaction. Aimed at this propose, we submitted (Au, Cu)/P25 to 355 and 532 nm laser excitation either purged with argon or in the presence of

quenchers ( $\text{O}_2$ ,  $\text{CH}_3\text{OH}$ ,  $\text{H}_2\text{O}$ , and  $\text{CO}_2$ ) and compare this behavior with that previously commented for Au/P25 and Cu/P25 samples. Figures 5 and 6 show transient spectra recorded for (Au, Cu)/P25 photocatalyst as well as a temporal profile of the signal monitored at 320 and 720 nm. Figure 5 also shows the linear dependency of the initial transient signal with the laser power (inset c), while Figure 6 compares the temporal profiles of the signal monitored at 480 nm upon excitation with low ( $33 \text{ mJ} \times \text{pulse}^{-1}$ ) and high ( $70 \text{ mJ} \times \text{pulse}^{-1}$ ) laser power (inset c). It has been commented that the decay of the signal was not influenced by the laser power for Au/P25 and Cu/P25, but upon excitation at 532 nm with the maximum laser power a certain variation of the decay with some growth at 5  $\mu\text{s}$  after the laser pulse was observed for (Au, Cu)/P25.

Decays monitored at either 320 or 720 nm show that in the case of (Au, Cu)/P25 the temporal profile of the signal is not significantly affected by the presence of these quenchers. Also, top  $\Delta J/J_0$  values are not affected by the presence of these quenchers when the irradiation is carried out at 355 nm. Overall, this quenching behavior observed for (Au, Cu)/P25 is very different to that of Au/P25, for which a large influence of the presence of quenchers in the intensity and on the profile of the signal was observed. The quenching behavior of (Au, Cu)/P25 was more alike, but not totally coincident, with that of Cu/P25 that does not become influenced by the presence of quenchers when irradiated a 532 nm monitoring at 320 nm in the presence of methanol.

With regard to the quenching behavior by water and  $\text{CO}_2$ , again the presence of water results in large changes that were different depending on the excitation wavelength. At 355 nm excitation, the presence of water increases the decay of the signal monitored either at 320 or 720 nm, while 532 nm excitation results in a dramatic change in the intensity of the top  $\Delta J/J_0$  value by a factor of 8. The influence of  $\text{CO}_2$ , on the transient spectra is similar, but not exactly coincident for (Au, Cu)/P25 and Au/P25. In this way, upon irradiation at 532 nm the presence of  $\text{CO}_2$  increases the intensity of the signal at all wavelength ranges, while UV irradiation increases the intensity of the signal corresponding to the 320 nm peak and it almost does not affect the signal monitored at 720 nm. Thus, under UV irradiation in the presence of  $\text{CO}_2$  (Au, Cu)/P25 exhibits in the long wavelength range of TAS an intermediate behavior between the quenching observed for Cu/P25 and the increase in signal intensity of Au/P25. Figure 7 provides a summary of the influence of  $\text{CO}_2$  and  $\text{H}_2\text{O}$  on the transient signals of (Au, Cu)/P25, depending on the excitation wavelength and the monitoring region.

As commented before, for the case of Cu/P25, the specific behavior in the quenching of (Au, Cu)/P25 by  $\text{CO}_2$  is the signal recorded upon 355 nm excitation monitored at 720 nm. Only for the transient signal recorded under this specific conditions and monitoring the long wavelength range, the signal of Au/P25 increases, the signal for Cu/P25 is quenched by  $\text{CO}_2$  and the signal for (Au, Cu)/P25 is almost unaffected by  $\text{CO}_2$ . It seems that, for these conditions, the response of (Au, Cu)/P25 is the average between the two contrasting behavior of Au/P25 and Cu/P25.

## CONCLUSIONS

In the present manuscript, the transient absorption spectra for three important photocatalysts with application in the field of solar fuels and specifically photocatalytic  $\text{CO}_2$  reduction by water have been studied. It has been found that, although the

TAS for the three samples containing metal NPs can be similar independently on the excitation wavelength, the behavior of the signal at different wavelengths in the presence of quenchers is different, depending on the nature of the metal NPs present on the surface of  $\text{TiO}_2$ . It has been found that the response of the transient signal is extremely influenced by the presence of quenchers, being either quenched or enhanced. In the particular case of  $\text{CO}_2$ , this gas has a general effect increasing charge separation and signal lifetime. The only evidence of  $\text{CO}_2$  quenching of electrons has been obtained for Cu/P25 photocatalyst upon irradiation in the UV and monitoring the broad 400–800 nm band. The sample (Au, Cu)/P25 exhibits in this region a behavior that is intermediate between that of Au/P25 and Cu/P25. Overall, our study shows the potential of TAS to understand and to rationalize the photocatalytic behavior of  $\text{TiO}_2$  modified with metal NPs as cocatalyst and the origin of the product selectivity. According to our study, irradiation with UV photons and the response introduced by Cu is what determines a distinctive behavior of this material derived from the transfer of CB electrons to  $\text{CO}_2$ .

## ASSOCIATED CONTENT

### Supporting Information

Transient spectra and temporal profile of the signals monitored at 320 or 720 nm and quenched by  $\text{O}_2$  or methanol as a function of the excitation wavelengths (355 or 532 nm) for P25, Au/P25, and Cu/P25 are presented. This material is available free of charge via the Internet at <http://pubs.acs.org>.

## AUTHOR INFORMATION

### Corresponding Author

\*E-mail: hgarcia@qim.upv.es.

### Notes

The authors declare no competing financial interest.

## ACKNOWLEDGMENTS

Financial support by the Spanish Ministry of Economy and Competitiveness (Severo Ochoa Grant CTQ 2012-3231S), the Deanship of Scientific Research (DSR), King Abdulaziz University, under Grant No. 75-130-35-HiCi, and Marie Curie Project PIEF-GA-2011-298740 is gratefully acknowledged. The authors acknowledge technical and financial support of KAU. We also thank the Generalidad Valenciana for postgraduate research contract to H.G.B. (Prometeo 2012/2013).

## REFERENCES

- (1) Amao, Y. Solar Fuel Production Based on the Artificial Photosynthesis System. *ChemCatChem* **2011**, *3*, 458–474.
- (2) Bolton, J. R. Solar Fuels. *Science* **1978**, *202*, 705–711.
- (3) Gust, D.; Moore, T. A.; Moore, A. L. Solar Fuels via Artificial Photosynthesis. *Acc. Chem. Res.* **2009**, *42*, 1890–1898.
- (4) Hammarström, L.; Hammes-Schiffer, S. Artificial Photosynthesis and Solar Fuels. *Acc. Chem. Res.* **2009**, *42*, 1859–1860.
- (5) Serpone, N.; Lawless, D.; Terzian, R. Solar Fuels: Status and Perspectives. *Sol. Energy* **1992**, *49*, 221–234.
- (6) Bahnemann, D. W. Current Challenges in Photocatalysis: Improved Photocatalysts and Appropriate Photoreactor Engineering. *Res. Chem. Intermediat.* **2000**, *26*, 207–220.
- (7) Fox, M. A.; Dulay, M. T. Heterogeneous Photocatalysis. *Chem. Rev.* **1993**, *93*, 341–357.
- (8) Herrmann, J. M. Heterogeneous Photocatalysis: Fundamentals and Applications to the Removal of Various Types of Aqueous Pollutants. *Catal. Today* **1999**, *53*, 115–129.

- (9) Neatu, S.; Macia-Agullo, J. A.; Garcia, H. Solar Light Photocatalytic CO<sub>2</sub> Reduction: General Considerations and Selected Bench-Mark Photocatalysts. *Int. J. Mol. Sci.* **2014**, *15*, 5246–5262.
- (10) Crabtree, G. W.; Dresselhaus, M. S.; Buchanan, M. V. The Hydrogen Economy. *Phys. Today* **2004**, *57*, 39–44.
- (11) Dunn, S. Hydrogen Futures: Toward a Sustainable Energy System. *Int. J. Hydrogen Energy* **2002**, *27*, 235–264.
- (12) Nowotny, J.; Sorrell, C. C.; Sheppard, L. R.; Bak, T. Solar-Hydrogen: Environmentally Safe Fuel for the Future. *Int. J. Hydrogen Energy* **2005**, *30*, 521–544.
- (13) Centi, G.; Perathoner, S. Towards Solar Fuels from Water and CO<sub>2</sub>. *ChemSusChem* **2010**, *3*, 195–208.
- (14) Liu, G. H.; Hoivik, N.; Wang, K. Y.; Jakobsen, H. Engineering TiO<sub>2</sub> Nanomaterials for CO<sub>2</sub> Conversion/Solar Fuels. *Sol. Energy Mater. Sol. C* **2012**, *105*, 53–68.
- (15) Morris, A. J.; Meyer, G. J.; Fujita, E. Molecular Approaches to the Photocatalytic Reduction of Carbon Dioxide for Solar Fuels. *Acc. Chem. Res.* **2009**, *42*, 1983–1994.
- (16) Corma, A.; Garcia, H. Photocatalytic Reduction of CO<sub>2</sub> for Fuel Production: Possibilities and Challenges. *J. Catal.* **2013**, *308*, 168–175.
- (17) Dhakshinamoorthy, A.; Navalón, S.; Corma, A.; García, H. Photocatalytic CO<sub>2</sub> Reduction by TiO<sub>2</sub> and Related Titanium Containing Solids. *Energy Environ. Sci.* **2012**, *5*, 9217–9233.
- (18) Chen, X.; Shen, S.; Guo, L.; Mao, S. S. Semiconductor-Based Photocatalytic Hydrogen Generation. *Chem. Rev.* **2010**, *110*, 6503–6570.
- (19) Primo, A.; Corma, A.; García, H. Titania Supported Gold Nanoparticles as Photocatalyst. *Phys. Chem. Chem. Phys.* **2011**, *13*, 886–910.
- (20) Haberreuter, S. N.; Schmidt-Mende, L.; Stolarsky, J. K. Photocatalytic Reduction of CO<sub>2</sub> on TiO<sub>2</sub> and Other Semiconductors. *Angew. Chem., Int. Ed.* **2013**, *52*, 7372–7408.
- (21) Neatu, S.; Macia-Agullo, J. A.; Concepcion, P.; Garcia, H. Gold-Copper Nanoalloys Supported on TiO<sub>2</sub> as Photocatalysts for CO<sub>2</sub> Reduction by Water. *J. Am. Chem. Soc.* **2014**, *136*, 15969–15976.
- (22) Baldoví, H. G.; Ferrer, B.; Alvaro, M.; García, H. Microsecond Transient Absorption Spectra of Suspended Semiconducting Metal Oxide Nanoparticles. *J. Phys. Chem. C* **2014**, *118*, 9275–9282.
- (23) Montes-Navajas, P.; Serra, M.; García, H. Influence of the Irradiation Wavelength on the Photocatalytic Activity of Au-Pt Nanoalloys Supported on TiO<sub>2</sub> for Hydrogen Generation from Water. *Catal. Sci. Technol.* **2013**, *3*, 2252–2258.
- (24) Navalón, S.; De Miguel, M.; Martín, R.; Alvaro, M.; García, H. Enhancement of the Catalytic Activity of Supported Gold Nanoparticles for the Fenton Reaction by Light. *J. Am. Chem. Soc.* **2011**, *133*, 2218–2226.
- (25) Kiselev, V. F.; Krylov, O. V. In *Springer Series in Surface Science*; Ertl, G., Gomer, R., Eds.; Springer-Verlag: Berlin, 1989; Vol. 9.
- (26) Martra, G. Lewis Acid and Base Sites at the Surface of Microcrystalline TiO<sub>2</sub> Anatase: Relationships between Surface Morphology and Chemical Behavior. *Appl. Catal., A* **2000**, *200*, 275–285.
- (27) Baltrusaitis, J.; Shuttlefield, J.; Zzeitler, E.; Grassian, V. H. Carbon Dioxide Adsorption on Oxide Nanoparticle Surfaces. *Chem. Eng. J.* **2011**, *170*, 471–481.
- (28) Liu, L.; Zhao, C.; Li, Y. Spontaneous Dissociation of CO<sub>2</sub> to CO on Defective Surface of Cu(I)/TiO<sub>2-x</sub> Nanoparticles at Room Temperature. *J. Phys. Chem. C* **2012**, *116*, 7904–7912.
- (29) Yang, C. C.; Hu, Y. H.; van der Linden, B.; Wu, J. C. S.; Mul, G. Artificial Photosynthesis over Crystalline TiO<sub>2</sub>-Based Catalysts: Fact or Fiction? *J. Am. Chem. Soc.* **2010**, *132*, 8398–8406.